Effect of charging-up and regular usage on performance of the triple GEM detector to be employed for plasma radiation monitoring

Maryna Chernyshova[a],*, Karol Malinowski[a], Tomasz Czarski[a], Iraida N. Demchenko[b], Yevgen Melikhov[c], Ewa Kowalska-Strzęciwilk[a], Andrzej Wojeński[d], Rafał D. Krawczyk[d,e]

[a] *Institute of Plasma Physics and Laser Microfusion, Hery 23, 01-497 Warsaw, Poland*
[b] *Laboratory of Electrochemistry, Department of Chemistry, University of Warsaw, Pasteura 1, 02-093 Warsaw, Poland*
[c] *School of Engineering, Cardiff University, CF24 3AA, Cardiff, UK*
[d] *Warsaw University of Technology, Institute of Electronic Systems, Nowowiejska 15/19, 00-665 Warsaw, Poland*
[e] *CERN, 1211 Geneva 23, Switzerland*

ARTICLE INFO

ABSTRACT

After the problem of high-temperature plasma confinement, construction of diagnostics that is able to identify plasma contamination with impurities and to determine impurity distribution is another critically important issue. Solution of this problem would enable progress towards the success in controlled thermonuclear fusion. A new diagnostics, based on Gas Electron Multiplier (GEM) technology, has been recently developed for poloidal tomography focused on radiation of the metal impurities by monitoring in Soft X-Ray (SXR) region. GEM based detectors would undergo much less damage by neutrons than standard semiconductor diodes which results in better operational stability. This paper emphasizes the results of the latest examination of this type of detectors, showing influence of the charging-up effect on the detector performance and its physical properties for expected plasma radiation intensity. In addition, an undesired influence of aging of the detector window's material on the performance of the GEM detector is also shown: regular (moderate or active) usage could lead to changes of material's morphology as well as its composition. This study confirms the importance of further research into material's optimization of GEM detectors used as a base for SXR tomographic diagnostics aimed to work under different plasma radiation conditions.

1. Introduction

After the problem of high-temperature plasma confinement, its contamination with impurities is another critically important problem, solution of which would allow continuation towards the success in controlled thermonuclear fusion. Basic information about impurities is obtained from studying their characteristic emission. The solution of most tasks within the problem of impurities depends, to a decisive degree, on the knowledge on the dynamics of the emission of impurities in time and space (over the cross section of the plasma core). Therefore, there is a need to develop diagnostics that suffers much less to a neutron damage than standard semiconductor diodes, and is able to reconstruct the impurity distribution.

Soft X-Ray (SXR) measurements is a well-established method to study diverse plasma physics phenomena. Having an appropriate tool for its monitoring, the obtained information could be very helpful in answering various plasma physics open questions as well as helping to

resolve plasma control issues. In magnetically confined devices plasma produces very intensive and anisotropic X-ray radiation in a wide energy region. Localization of the emission in a certain plasma volume is associated with requirement of a high dynamic range in the detecting system, so it is able to discriminate radiation differing in intensity by orders of magnitude. Recently, aiming for the future thermonuclear reactors, new type of the detectors has been proposed for plasma physics application [1–3].

The proposed type of detectors, Gas Electron Multipliers (GEMs) [4], is based on gaseous multiplication of the primary signal originated from the incoming ionizing radiation passed through the gaseous media. A typical triple-GEM detector has a sandwich-like structure: a detector window (that serves as a cathode), three GEM foils, each with Cu layers deposited on both sides (serving as electrodes) and readout plane (that serves as an anode). A set of voltages is then applied to all electrodes. Since each GEM foil contains a net of holes, voltages applied to Cu layers form a dipole-like high electric field in these holes. On the

---

other hand, voltage difference between parallel constituents of the detector results in a parallel electric field regions. The superposition of parallel and dipole-like electric fields creates the net electric field of the device.

Generally, the detector amplification, and therefore photon energy estimation, directly depends on the applied voltage difference between the GEM foil's electrodes. However, since GEM foil uses an insulating Kapton film as a base, a charging-up effect has to be taken into account as well. Charge accumulation on the dielectric surface leads to a distortion of the originally applied electric field, which in turn leads to a modification of the amplification under the stuck charge. Despite an obvious importance of this effect, one can achieve a long-term stable effective amplification factor after an essential (but relatively short) amount of time.

Variation of plasma radiation conditions on a long term will be affecting an amplification factor due to variation of the stuck charge. Moreover, besides standard external factors such as pressure and/or temperature, other factors may influence the amplification factor on a long-term usage of GEM detectors. In this work we continue investigations of properties of GEM detectors used as a base for SXR tomographic diagnostics aimed to work under different plasma radiation conditions. We present and analyze time dependent measurements of the amplification for the detectors that are just produced and the detectors that have been either moderately or actively used.

2. Results and discussion

2.1. Experimental details

Standard triple-GEM detector structure is used in this study. Three standard GEM foils, manufactured at CERN following basic CERN routines, either with double conical (70/50 μm of outer/inner diameter) or cylindrical (70 μm diameter) holes with 140 μm pitch are employed. The detector window is a Mylar foil of 5 μm thickness metalized by $30-40$ nm thick Al layer. The gas medium of 0.1 L total volume was Ar/CO_2 at the ratio of 70/30 with 50 mL/min flowing rate. Values of applied voltages and/or electric field in the drift gap are specified in subsequent sections. The detector effective gain was determined using either pulse-height [5–7] or detector's current recording techniques [8].

Altogether, four GEM detectors were experimentally studied that differ by the hole shapes and/or time of usage. Two "fresh" detectors with different hole shapes were produced just before the experimental work. Moderately used GEM detector with cylindrical holes and actively used GEM detector with double-conical holes have been in operation for several years.

2.2. Effective gain of the moderately/actively used triple-GEM detector monitored in a short time-scale

It is well known that the charging-up effect on the dielectric surfaces causes the changes of the GEM detector amplification due to the charges being accumulated on the Kapton surface within GEM holes (see, e.g., [9,10] for experimental and [11–13] for theoretical studies). If a substantial number of charges is collected on the dielectric surfaces, it starts modifying the electric field inside the GEM holes. This leads to a variation of the detector performance with time even in case of a constant flux of ionizing radiation *and* constant high voltage applied to the GEM foils, as shown in Fig. 1. It needed about 1 μC/cm^2 of the detector total charge density (on the reading electrode) for reaching stabilization of the detector's gain, and that, at a very low counting rate (about 0.4 Hz/mm^2) being used, could last several hours. In the literature this effect was reported to be of more or less 20% of the gain increase measured with standard GEM foils [9,10].

Based on the understanding of the charging-up effect, the gain increase should practically be insignificant in GEMs with cylindrical holes
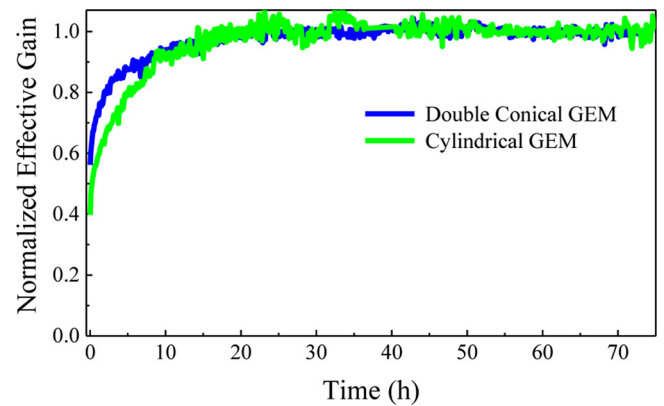

Fig. 1. Initial gain increase as a function of time for the moderately/actively used triple-GEM detectors with double-conical and cylindrical holes at low radiation rate for 370 V applied to all GEM foils.

[10,13]. This is due to the fact that for such a shape, there is no dielectric surface exposed in the holes for a back-drifting charge, and therefore, it is very unlikely that back-drifting charge will end up on a surface of the hole [9,14].

Our measurements, however, show the total growth of the gain of far more than 20%, even for the cylindrical holes, what is in obvious contradiction with the literature data. In order to identify the reason for this behavior, further measurements were designed and performed.

2.3. Variation of the effective gain under exposure to high intensity SXR radiation

Modification and evolution of the detector's effective gain was measured under high intensity radiation shown in Fig. 2. As the X-ray tube voltage was kept the same, varying the applied current should cause the rise of the intensity only. Nevertheless, as can be observed in Fig. 2, the peak position (effective gain of the detector) of the gathered spectrum shifts to lower values with the higher radiation intensity.

The spatial distribution of the detector amplification before and after the irradiation is presented in Fig. 3. The medium-term effect of the applied radiation was revealed in the pronounced gain drop for the irradiated part of the detector within pixels $20-60$. This effect lasted for more than two weeks until its full recovery, examined at a very low rate by means of ^{55}Fe source measurement.

The restoration of the effective gain took much more time than expected for this type of detectors built with the GEM foils ordered from
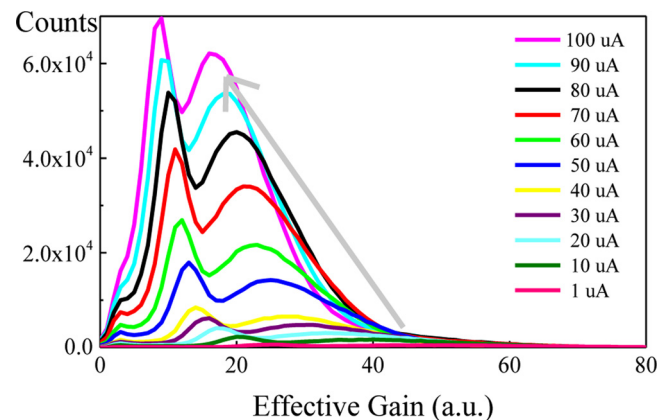

Fig. 2. Spectra taken under irradiation of the standard triple-GEM detector, supplied by 370 V at each GEM foil, by X-ray tube of the same voltage applied and various current (different radiation intensity up to about 0.6 kHz/mm^2 for the highest X-ray tube current).
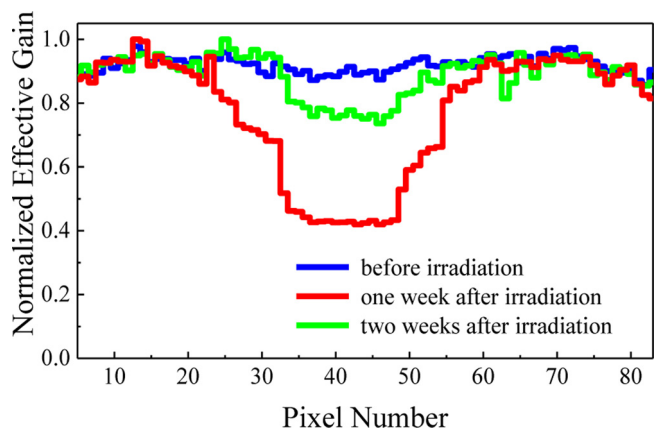
Fig. 3. Modification and evolution of the effective gain, gathered using low intensity ^{55}Fe source, of the moderately used detector under high intensity SXR radiation.

CERN. To explain the observed behavior, conditions at the drift gap, i.e. under detector window, were investigated.

2.4. Influence of conditions at the drift gap on the "fresh" and moderately/ actively used triple-GEM detectors: simulation vs. experiment

The electric conditions at the drift gap are controlled via the voltage difference between a cathode on a detector window (Al layer) and the top electrode of the first GEM foil (Cu layer). Since the layers are parallel to each other (due to sandwich-like structure of the GEM detector) and since the thickness of the drift gap is kept the same for such a detector (typically the thickness is $2-10$ mm with 5 mm in this case), the electric field can be easily estimated even under experimental conditions. This would allow a straightforward analysis of the effect of changes of the electric field in the drift gap on the detector gain both experimentally and numerically.

In addition, due to being interested in the drift gap only, numerical simulation of a single-GEM detector configuration is sufficient. In this case, the following parameters were chosen: drift gap (5 mm)/standard double conical or cylindrical GEM foil/transfer gap (2 mm). The voltage on the GEM foil was set to 380 V, and the electric field on the transfer was kept at the value of 1200 V/cm. The voltage on the drift ranged from 200 V/cm to 4500 V/cm in steps of 100 V/cm. In this way, 44 configurations of electric field in the detector chamber were obtained. Calculations were performed for each configuration using the Monte-Carlo method using Garfield++, simulating the avalanches arising from 10^5 primary electrons. The charging-up effect was not incorporated into simulation. Amplification was calculated as the ratio of the number of primary electrons to the number of electrons on the reading electrode (i.e., after transfer).

Besides numerical simulations, measurements under the same conditions in the drift gap were performed for all four triple-GEM detectors: "fresh" (with double-conical and cylindrical holes) as well as the moderately (with cylindrical holes) and actively used (with double-conical holes).

Comparison of numerically simulated and experimentally obtained effective gain as a function of the drift electric field is presented in Fig. 4. There is an obvious substantial discrepancy in the behaviors of simulated and actively used GEM detector with the double-conical holes. This discrepancy is present, to a much lesser extent, in case of simulated and moderately used GEM detector with the cylindrical holes, which are in accordance with [14].

Generally, under the applied experimental conditions of laboratory testing, the integral charge flow was less than 1 C/cm^2 [15,16]. Therefore, there should not be any damage effects of such an integral charge onto GEM foils of CERN production. This allows us to exclude an
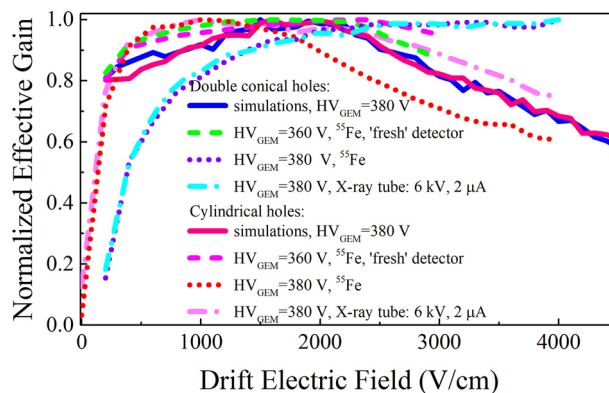
idea that the observed discrepancy is related to GEM foils.

This leaves us with the assumption that the detector window itself is responsible for deterioration of the detector performance. In order to confirm that, high intensity radiation (at constant irradiation flux, resulting in counting rate up to about 4.5 kHz/mm^2) was applied to two different spots on the surface of the same detector differing only by the applied electric field at the drift gap. The results, shown in Fig. 5, provide an evidence that the detector window negatively affects the amplification of the detector. Considering that the incoming intensity was below the space charge accumulation limit for the GEM detectors, it can be assumed that the detector window, serving as the cathode of the structure, does not provide sufficient conductivity and, therefore, charges agglomerate on its surface. Spatial distribution of the effective gain over the detector's surface obtained by means of ^{55}Fe source revealed a distinction between two initially irradiated areas (at high radiation flux applied) at different drift gap electric fields. The measurements were taken just after the irradiation and in three days time (see Fig. 6). As can be observed the collected charge, that lead to an undesired modification of the electric field, was initially lower and eventually recovered quicker for higher value of the high voltage applied to the detector window. The confirmation of the local charging-up effect on the surface of the detector window was achieved for this measurement.

This assumption was checked on the actively used detector with double-conical holes that was subjected to a 'rough' uncharging, i.e. it was switched off for a few days with the flowing gas only. In this experiment, the same position of the detector of about 1 cm^2 was irradiated by X-ray tube generating constant flux, resulting in the counting rate of approximately 40 kHz/mm^2, keeping the same conditions except
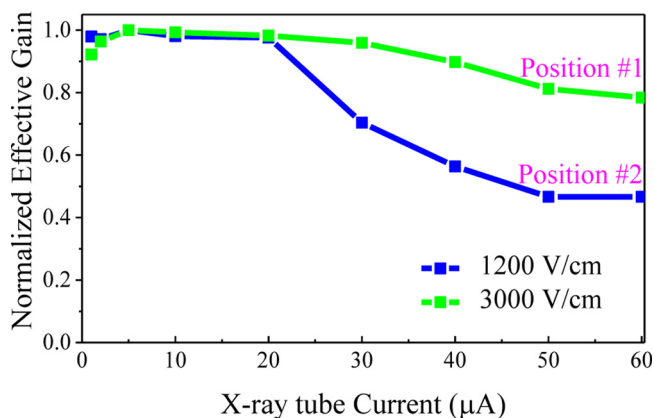

Fig. 4. Drift field dependencies of the effective gain for "fresh" and moderately/ actively used triple-GEM detectors with double-conical and cylindrical GEM holes, as well as for (numerically simulated) a single-GEM detector.

Fig. 5. Modification of the effective gain for "fresh" double-conical detector's under irradiation of X-ray tube for two values of the drift electric field.
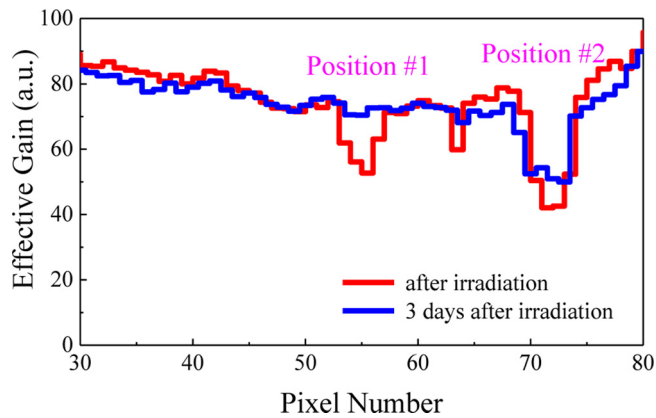
Fig. 6. Spatial distribution of the effective gain for "fresh" double-conical triple-GEM detector after irradiation at different drift electric fields.
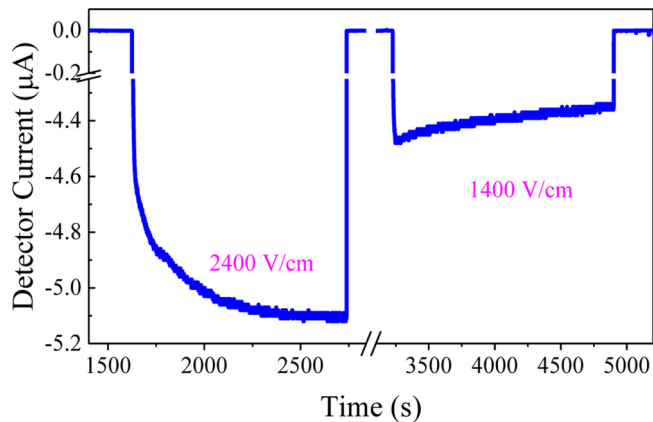

Fig. 7. Time dependence of the uncharged detector current under irradiation by X-ray tube for two different drift electric fields.

for two different electric fields applied to the drift gap. The total current of the detector was measured by the pico-ammeter (Keithley 6487) through the $100 \text{ k}\Omega$ protecting resistor. As shown in Fig. 7, for higher potential the time dependence at the very beginning of the exposure resembles a charging-up effect that was observed for the detector (see Fig. 1): the detector amplification growth with time, i.e. total detector current increase under the constant incoming radiation. In the case of the lower potential, when all the other conditions were kept the same as for the higher potential, the detector amplification was initially decreasing, manifesting the comparable opposing impact of the window charging-up effect.

Taking all of the above into account, the detector window's material was further examined for the possible changes in its composition and/

or morphology that resulted from its usage.

3. Examination of structural changes of the detectors' window

The detector window used to construct the triple-GEM detectors in this work is a quite common detector window used for SXR measurement purposes: a Mylar foil of 5 μm thickness is taken as a base that is coated by $30-40 \text{ nm}$ thick Al layer to serve as a cathode. Due to its nature, Aluminum quickly oxidizes into alumina Al_2O_3, and a very thin layer of a *stable* alumina is formed preventing further oxidation. At considered operational temperatures, and up to even 300 C, alumina is an electric insulator [17]. Nevertheless, since the alumina layer is very thin, this only adds a contact resistance not interfering with the further layer of Al that remains a perfect conductor (note that conductivity through such a thin layer occurs via the effect of tunneling).

For the preliminary tests of the detector window, pieces from the actively exploited detector window and from a non-used ("virgin") aluminized Mylar foil (ordered from Goodfellow Cambridge Ltd, UK) were studied by Scanning Electron Microscope (SEM) and X-ray Photoelectron Spectroscopy (XPS) techniques.

First of all, field-emission SEM (Merlin, Carl Zeiss) at operating voltage of 3 kV was applied to examine the morphology of the samples. A composition of the aluminized Mylar foil was also determined from EDX elemental analysis (at accelerating voltage of 15 kV). The images of the non-used and used foils, shown in Fig. 8, reveal some changes that occurred in the foil that was used as a detector window. Namely, regions of the detector window that were stripped of Al, i.e. regions of the uncovered Mylar foil (seen as dark spots of the carbon tape that is visible through transparent Mylar foil), slightly grew in size/quantities after utilization. We assume, that besides the effect of limitation on amplification and the secondary effect of field distortion, avalanches of ions moving in the opposite direction to electrons are the destructive factors for the thin aluminum cathode that determines its aging.

The samples were studied by XPS technique using AXIS Supra spectrometer with monochromatic Al K_α radiation (1.4866 keV) from an X-ray source with a spot of $700 \times 300 \text{ μm}^2$ (due to the analyzer settings in hybrid mode) while operating at 150 W. The High-Resolution (HR) XPS spectra were collected with the hemispherical analyzer at the pass energy of 20 eV and the energy step size of 0.1 eV. The photoelectron take-off angle was 0° with respect to the normal to the sample's surface plane. An analyzer acceptance angle was $\pm$ 7°. The charge compensation was applied. Samples were mounted on the grounded holder. Binding Energies (BEs) of the photoelectrons were calibrated using the carbon 1 s photoelectron peak at 285 eV. The CasaXPS software (version 2.3.17) [18] was used to evaluate the XPS data.

XPS was performed to gain insight into the position of core levels of the atoms present in the surface region (about 10 nm thick) of the investigated samples. After control measurement of a wide spectrum, the
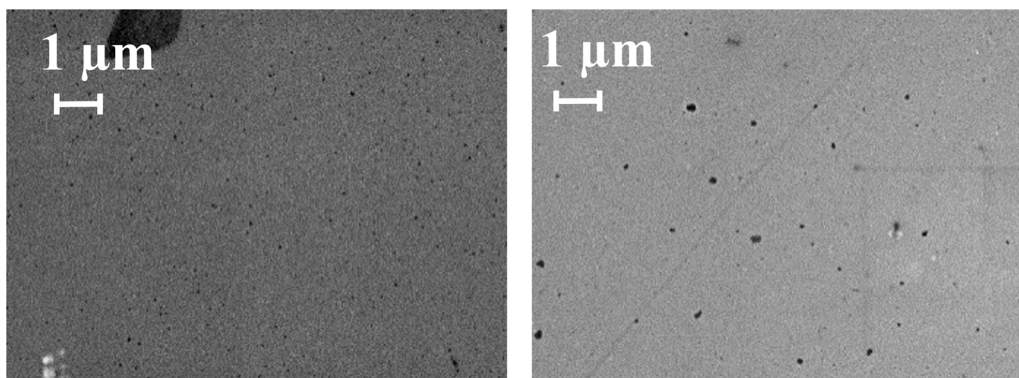

Fig. 8. SEM images of the aluminized Mylar surface before (left) and after (right) application in triple-GEM detector.
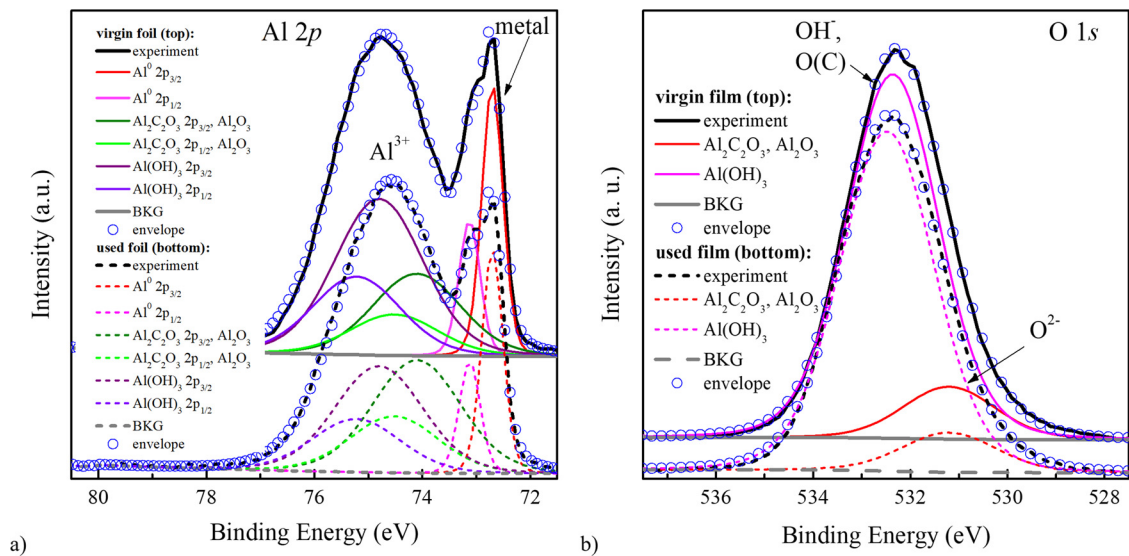
Fig. 9. Aluminum 2p (a) and oxygen 1s (b) photoelectron spectra measured for Al/Mylar tapes before and after work treatment (marked as "virgin" and "used," respectively).

HR XPS spectra of the Al 2p, O 1s, C 1s, N 1s, F 1s peaks were obtained for the aluminized Mylar films before and after exploitation as detector windows (marked below as "virgin" and "used", respectively). Prior to the analysis, an adventitious C 1s peak (at 285 eV) calibration of the BE was executed.

Fig. 9 (a) shows comparison of the HR Al 2p core-level XPS spectra measured from "virgin" and used films. The Al signal revealed two peaks representing the oxide and metal states. The doublet spectral lines of Al 2p were observed at the BEs of 72.70 ± 0.15 eV ($2p_{3/2}$) and 73.12 ± 0.15 eV ($2p_{1/2}$) with a spin-orbit splitting of 0.42 eV, which coincides with the results for Al 2p in Al metal [19], whereas, BEs at 74.10 ± 0.15 eV (Al^{3+} $2p_{3/2}$) and 74.80 ± 0.15 eV (Al^{3+} $2p_{3/2}$) correspond to Al_2O_3 and $Al(OH)_3$ phases [19], respectively. Thus, the chemical shifts are 1.4 and 2.1 eV. The oxygen signal of the samples reveals high-intensity slightly asymmetric peak representing O^{2-} in Al_2O_3 at 531.20 ± 0.15 eV and OH^- in $Al(OH)^3$ at 532.37 ± 0.15 eV, respectively, see Fig. 9 (b). The obtained values agree well with the literature [20].

For the "virgin" film, the measured intensity ratio of Al_2O_3 to metal aluminum is 1.3 and for $Al(OH)_3$ to Al^0 it is 2.4, whereas total oxide signal (Al_2O_3 + $Al(OH)_3$) to metal one (Al^0) is 3.7. These ratios for the used film are: 2.6, 2.0 and 4.5, respectively, manifesting an expansion of the alumina layer in the used foil as compared to the foil that has not been used. The higher $Al(OH)_3$ fraction in the "virgin" foil could be related to longer stay at the air atmosphere, compared to the used foil.

The intensity ratio between the intensities of the oxide and metal peaks was, then, used in the Strohmeier equation [21,22], showing the oxide thicknesses of 50.7 Å (for the "virgin" foil) and 55.7 Å (for the used foil).

Let us note that the carbon spectra (data are not presented there) show peaks representing bonds C-C/C-H, C-O-C/C-OH, O-C=O, within $Al_2C_2O_3$ and C=O at BEs of 285, 286.13, 289.83, 283.70 and 287.23 ± 0.15 eV, respectively. It was also found that comparatively to the "virgin" foil (where N 1s signal is missing), the used film reveals N 1s peak at 399.62 ± 0.15 eV of BE which could be interpreted as nitrogen bonded to surface C=O group. Moreover, the F signal at 686.40 ± 0.15 eV of BE was also discovered to be higher for the used film. This may be due to the interaction of the window surface with the working gas in the detector (in this case another quenching agent, CF_4, was used for the laboratory tests).

4. Summary

Application of GEM detectors in plasma physics requires its operation with high rate capability, close to its space charge limit ($\sim 10^5$ Hz/mm^2). At such corresponding current density flowing through the detector, the charging-up effect of all existing in the detector insulating surfaces should be taken into account for its stable operation. This is, for example, due to the fact that ionic reverse current to preceding GEM foils and to the cathode could lead to charging the dielectric surfaces at high anode current densities and, thus, creating gain instability.

Here we showed that charging-up effect on the detector window clearly affects the detector's effective gain. It was also shown that there is an undesired influence of aging of the detector window's material on the performance of the GEM detector: regular (moderate or active) usage could lead to changes of material's morphology as well as its composition. To resolve this issue, considering that SXR radiation recording expects application of light-Z materials, the usage of thicker Al layer, either commercial off-the-shelf or custom made, might be considered. In addition, since thin alumina layer is formed straight away on Al conductor, this layer itself may add up to a charging-up effect. Therefore, exploitation of low oxidation materials and/or new materials, such as, graphene layers or diamond-like carbon coatings, for detector window suitable for SXR measurements could also be considered.

Overall, this study confirms the importance of further research into material's optimization of GEM detectors used as a base for SXR tomographic diagnostics aimed to work under different plasma radiation conditions.

CRediT authorship contribution statement

Maryna Chernyshova: Conceptualization, Investigation, Methodology, Supervision, Validation, Writing - original draft, Writing - review & editing. **Karol Malinowski:** Software, Data curation, Investigation. **Tomasz Czarski:** Software, Data curation, Formal analysis. **Iraida N. Demchenko:** Investigation, Validation, Visualization, Formal analysis. **Yevgen Melikhov:** Investigation, Writing - review & editing. **Ewa Kowalska-Strzęciwilk:** Visualization. **Andrzej Wojeński:** Data curation. **Rafał D. Krawczyk:** Data curation.

Declaration of Competing Interest

Acknowledgments

References

[1] D. Mazon, et al., GEM detectors for WEST and potential application for heavy impurity transport studies, JINST 11 (2016) C08006.

[2] M. Chernyshova, et al., Development of GEM gas detectors for X-ray crystal spectrometry, JINST 9 (2014) C03003.

[3] F. Cordella, et al., Results and performances of X-ray imaging GEM cameras on FTU (1-D), KSTAR (2-D) and progresses of future experimental set up on W7-X and EAST Facilities, JINST 12 (2017) C10006.

[4] F. Sauli, The gas electron multiplier (GEM): operating principles and applications, Nucl. Instrum. Methods Phys. Res. A 805 (2016) 2–24.

[5] T. Czarski, et al., The cluster charge identification in the GEM detector for fusion plasma imaging by soft X-ray diagnostics, Rev. Sci. Instrum. 87 (2016) 11E336.

[6] A. Wojenski, et al., Concept and current status of data acquisition technique for GEM detector based SXR diagnostics, Fusion Sci. Technol. 69 (2016) 595.

[7] T. Czarski, et al., Data processing for soft X-ray diagnostics based on GEM detector measurements for fusion plasma imaging, Nucl. Instrum. Methods Phys. Res. B 364 (2015) 54.

[8] M. Chernyshova, et al., Study of the optimal configuration for a Gas Electron Multiplier aimed at plasma impurity radiation monitoring, Fusion Eng. Des. 134 (2018) 1–5.

[9] J. Benlloch, et al., Further developments of the gas electron multiplier (GEM), Nucl. Instrum. Methods Phys. Res. A 419 (1998) 410.

[10] B. Azmoun, et al., A study of gain stability and charging effects in GEM foils, Nucl. Sci. Symp. Conf. Rec. IEEE 6 (2006) 3847–3851.

[11] M. Alfonsi, et al., Simulation of the dielectric charging-up effect in a GEM detector, Nucl. Instrum. Methods Phys. Res. A 671 (2012) 6–9.

[12] P.M.M. Correia, et al., A dynamic method for charging-up calculations: the case of GEM, JINST 9 (2014) P07025.

[13] V. Tikhonov, R. Veenhof, GEM simulation methods development, Nucl. Instrum. Methods Phys. Res. A 478 (2002) 452–459.

[14] S. Bachmann, et al., Charge amplification and transfer processes in the gas electron multiplier, Nucl. Instrum. Methods Phys. Res. A 438 (2-3) (1999) 376–408.

[15] L. Guirl, et al., An aging study of triple GEMs in Ar-CO2, Nucl. Instrum. Methods Phys. Res. A 478 (2002) 263.

[16] C. Altunbas, et al., Aging measurements with the gas Electron multiplier (GEM), Nucl. Instrum. Methods Phys. Res. A 515 (2003) 249.

[17] J.F. Shackelford, et al., CRC Materials Science and Engineering Handbook, 4th ed., CRC Press, 2015.

[18] http://www.casaxps.com.

[19] http://www.xpsfitting.com/search/label/Aluminum.

[20] https://srdata.nist.gov/xps/main_search_menu.aspx.

[21] T.A. Carlson, G.E. McGuire, Study of the x-ray photoelectron spectrum of tungsten—tungsten oxide as a function of thickness of the surface oxide layer, J. Electron Spectros. Relat. Phenom. 1 (2) (1972) 161–168 1973.

[22] B.R. Strohmeier, An ESCA method for determining the oxide thickness on aluminum alloys, Surf. Interface Anal. 15 (1990) 51–56.